IOSR Journal of Mechanical and Civil Engineering (IOSR-JMCE)
e-ISSN: 2278-1684,p-ISSN: 2320-334X, Volume 20, Issue 2 Ser. III (Mar. – Apr. 2023), PP 42-57
www.iosrjournals.org

Performance Analysis of Combined Cycle Power Plant with Inlet Air Cooling System

Mude Murali Mohan Naik[1], Dr. V. S. S. Murthy[2], Dr. B. Durga Prasad[3]
[1]*Research Scholar, Department of Mechanical Engineering, JNTUA, Anantapuramu, INDIA.*
[2]*Professor & Principal, KSRM College of Engineering, Kadapa, INDIA*
[3]*Professor, Department of Mechanical Engineering, JNTUACE, Anantapuramu, INDIA*

ABSTRACT
Combined Cycle power Plant (CCPP) is utilized for generating electricity. It is a highly effective and efficient generation unit of power. However, the overall performance of CCPP depends on the inlet air temperature. Hence, in this paper, an inlet air cooling system based on Lithium Bromide-Water (LiBr/H_2O) are investigated and the thermodynamic model was analyzed. Moreover, a novel Hybrid Ant Colony Bat Absorber system (HACBAS) was developed to optimize the developed model. Based on this approach, the system coefficient of performance (COP) is improved. The simulation model of CCPP absorption system is carried out with MATLAB.
Keywords: Combined cycle power plant, Hybrid Ant Colony Bat Absorber system, inlet air cooling system, Lithium Bromide-Water.

Date of Submission: 10-04-2023 Date of Acceptance: 23-04-2023

I. INTRODUCTION

Electrical energy is an important input towards the development of a country's economy. About ninety five percent of the world's energy requirements come from the fast depleting fossil fuels. In this direction thermal power plant capacity addition is being augmented by efficient modes of power generation such as coal based supercritical power plants and gas based combined cycle power plants.

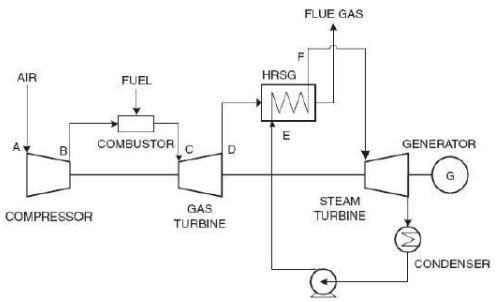

Fig.1 Combined cycle power plant

Many researchers try to solve the problem by a variety of methods hybrid turbine by inlet air cooling (TIAC) system, Brayton Rankine Combined-cycle power plant (CCPP) [1], ORC-ARS system etc. [2]. In past, several vapour absorption model was implemented, but those model have been attained less thermal efficiency range. For that inlet air cooling system was introduced in the CCPP model [3] .Two cycles of thermodynamics are of Steam and gas turbine cycle combine to form the CCPP [4]. To form the efficient combined power cycle, two cycles are a complement to each other [5]. High-temperature resource requires for the Brayton cycle and high-temperature discharge source is used forthe Rankine cycle [6].

Two main types of inlet air cooling method 1.water evaporation systems 2.heat transfer system. Water evaporation consist of two processes is inlet fogging and evaporative cooling, here temperature will decrease directly [7]. Heat transfer system decreases air temperature indirectly to the power plant situated area, weather condition, etc. [8]. Power generation and CCPPs depend on the gas turbines. Their cost is less, compact size, the flexibility of fuel, lightweight, and low emission [9]. Moreover, several works are done in the past like Hybrid sorption-vapor and compression cooling system [10], wastage of heat energy [11], Integrated Cooling System with CCPP [12], etc. But still, there is no improvement in increase of heat absorbance. These issues were motivated towards this research.

II. RELATED WORKS

Some of the possible literature associated with a CCPP by inlet air cooling, vapour absorption in refrigeration system is summarized below

Mohamed G. Gado*et al* [13] have analyzed Hybrid sorption-vapor and compression cooling system, heat from the condenser sent into absorption and adsorption chillers, and significant amount of heat is given to the desorber therefore no need to direct heat for the chillers. The main advantage is accurate temperature with a high speed response, suitable for humid and hot temperature.The main disadvantage is size is very large, lack of moving parts and more time taken to introduce into the market.

Organic Rankine Cycle (ORC) is used for generating power Wastage of heat energy from the diesel engine, used for refrigeration by absorption-based refrigeration system (ARS) and the adsorption-based cooling system (ACS). A. M. Alklaibi and N. Lior [14] proposed the method wastage of heat energy is utilize for the purpose of power generator and refrigeration.Fuel consumption is reduced 5-11.3%,thermal efficiency is increase up to 5%. ORC-ARS system improved 3% heat recovery.

To meet the high peak load in summer Khaliq and Dincer [15**]** have analyzed combined energy and heat for the power plant by inlet cooling absorption and evaporative after cooling. It is reported that in combustion chamber, heat recovery steam generator, generative heat exchanger most of the destruction cycles are happen. The overall efficiency and ratio influence by the energy efficiency and power to heat ratio of the cycle.75 % of exergy destruction during the combustion.

Wei Peng and Omid Karimi Sadaghiani [16] introduced Integrated Cooling System, with CCPP to reduce the water temperature from the condenser. ORC is connected with Hellen cooling tower to improve the cooling capacity. This method can decrease water temperature from 313K to 303K.This method canimprovecooling capacity of hellen tower. More power is generated by stability of cooling system. Exergy efficiency rate is 37.59%. This parameter increases from 20.04% to 21.94%, optimization of the system increase of the capital costs.

Adnan Darwish Ahmad *et al* [17] have analyzed integration of hybrid inlet cooling & solar systems. The flue gas produce energy from the CCPP is combined with power generator. Flue gas from gas turbine directed to the heat recovery generator it increases the temperature, where flow is separated into stream. By this method power is increase up to 22.8% and increase in efficiency of 4.3% and fuel consumption decreased by 8.4 %. Capital cost is high.

III. SYSTEM MODEL AND PROBLEM DESCRIPTION

The combine cycle power plant (CCPP) system have both steam and gas turbines for network power supply. The system model of the CCPP is represented in fig.2.

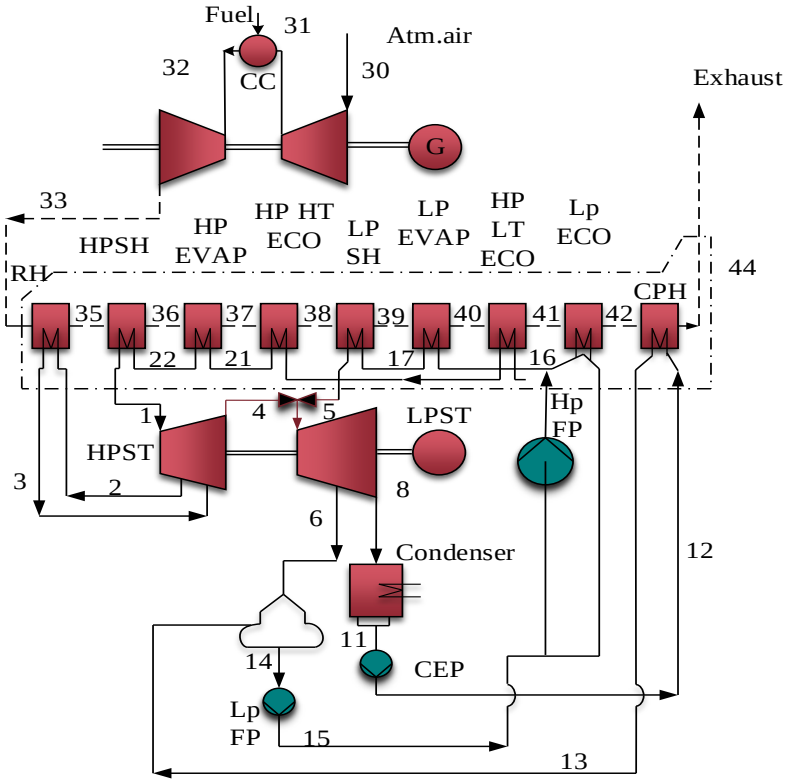

Fig.2 System model

The steam and gas turbine was utilized in CCPP for electricity production. Where, HP represents the high pressure; LP is the low pressure; HT is the high temperature; LT represents the low temperature; GT denotes the gas turbine; ST represents the steam turbine; RH is the re-heater; SH is the super heater; EVAP denotes the evaporator; eco is represented for economizer; CPH is denoted for condensate pre-heater; FP is the feed pump; CEP is the condensate extraction pumps.

IV. PROPOSED HYBRID ANT COLONY BAT ABSORBER SYSTEM (HACBAS)

To optimize the heat absorber to attain the best cooling capacity and electricity producing level, the present article has aimed to design a novel hybrid optimization strategy that is known as Hybrid Ant Colony Bat Absorber system (HACBAS). By implementing the proposed methodology, the required amount of heat is taken for cooling purpose and other waste heat is utilized to produce electricity. The proposed architecture is detailed in fig.3

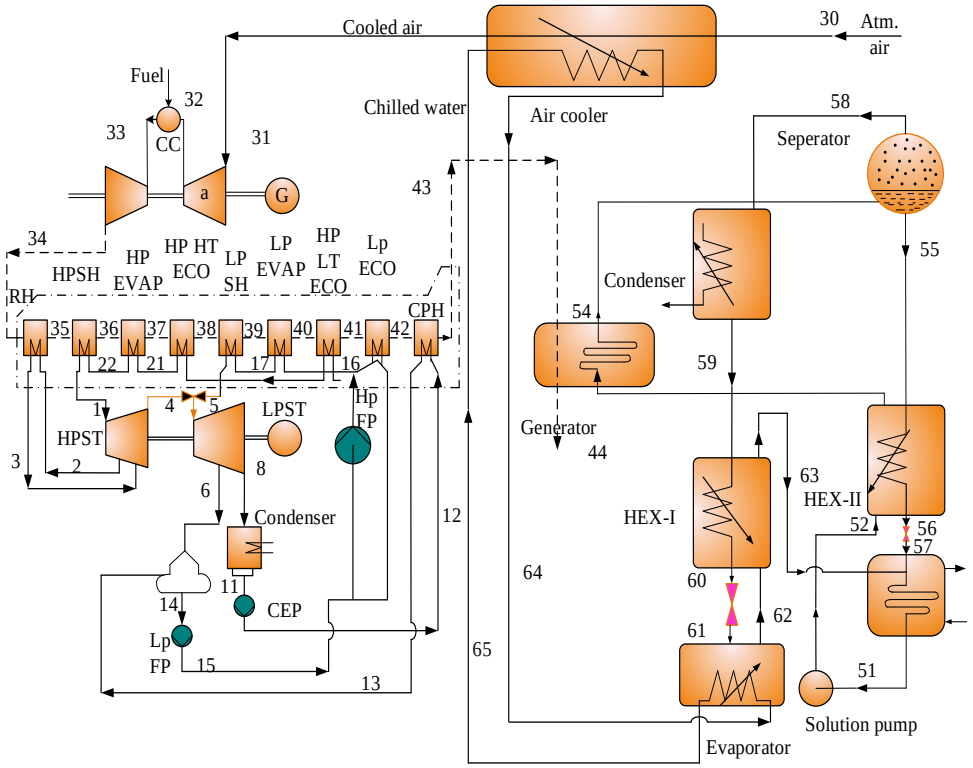

Fig.2 proposed methodology

HRSG represents the heat recovery steam generator and HEX is the heat exchanger. In CCPP, the main purpose of HRSG is utilized to recover the heat from the GT hot gases to generate steam for the ST. The HRSG contains four components i.e. super heater, water preheater, evaporator and economizer. Moreover, based on the pressure levels, it is categorized into multi pressure or single pressure. Here dual pressure is utilized in the proposed HRSG.

4.1 Thermodynamic model of air cooling and integrated power system

In the presented CCPP model, the GT plant is provided in top of the power plant and ST plant is provided in bottom of the power plant. These two plants were coupled with a HRSG with dual-based pressure. To cool the inlet air, Lithium Bromide (LiBr)/water (H_2O) in single effect Vapour absorption Refrigeration (VAR) system was provided. To decrease the atmospheric temperature of air, the cooling system evaporator is combined with air cooler. The chilled water circuit was placed between the air cooler and evaporator heat exchangers for transferring the heat from the cooling coil to air. In the gas plant stack, the heat recovery system provides energy to the VAR cooling system. It works as a lower grade thermal source of energy for the cooling supplying system about 80^0C-130^0C.

From pressure ratio, the GT and compressor isentropic efficiency is evaluated and it is expressed in eqn. (1) & eqn. (2).

GT's isentropic efficiency, $$\delta_{GT} = \frac{1-\left(\frac{S_{33}}{S_{32}}\right)^{\frac{\delta_{\infty GT}(\tau-1)}{\tau}}}{1-\left(\frac{S_{33}}{S_{32}}\right)^{\frac{(\tau-1)}{\tau}}} \quad (1)$$

Compressors isentropic efficiency, $$\delta_C = \frac{P_r^{\left(\frac{\tau-1}{\tau\delta_{\infty C}}\right)}-1}{P_r^{\left(\frac{\tau-1}{\tau}\right)}-1} \quad (2)$$

Where, δ_{GT} and δ_C represents the GT and compressor isentropic efficiency respectively, P_r denotes the pressure ratio, S denotes the polytrophic relation, δ_∞ represents the efficiency of polytrophic state, τ represents the ratio of specific heat, $\delta_{\infty GT}$ and $\delta_{\infty C}$ denotes the polytropic efficiencies of GT and compressor respectively. The modeling of CC system was started with a selected deaerator-based pressure. The saturated liquid is a exist state of deaerator and from the temperature of saturation, the LP is determined. By heat balance equations, the heating devices of steam's flow rate and gas temperature is determined. The LP evaporator saturation temperature is evaluated using eqn. (3)

$$ST^*_{LP} = T^*_{LPexit} - DSH_{LP} - TTD_{LP} \quad (3)$$

The flue gas outlet temperature at HP evaporator, $T^*_{36} = ST^*_{HP} + PP_{HP}$ (4)

The flue gas outlet temperature at LP evaporator, $T^*_{39} = ST^*_{LP} + PP_{LP}$ (5)

The water outlet temperature r at HP, HT economizer, $T^*_{21} = ST^*_{HP} - AP_{HP}$ (6)

The outlet temperature of water at LP economizer, $T^*_{16} = ST^*_{LP} - AP_{LP}$ (7)

Where, ST represent the saturation temperature. The interaction of works in steam and gas cycles is computed to fuel unit mass. For analysis of exergy, the irreversabilities in all the components are estimated to measure the exergetic losses. For this analysis, the losses and efficiency are evaluated for fuel with 1kmol. The fuel exergy and chemical availability was the maximum attained theoretical work by allowing the fuel to correlate with environment-based oxygen to generate water vapor and carbon dioxide environmental components. In the gas combustor based on fuel, the chemical contribution plays a vital role and the components chemical exergy are evaluated for each state by eqn. (9).

Chemical exergy, $$E_{ch} = \sum_m n_m \varepsilon^0_m + RT^*_0 \sum_m n_m \, ln[Px_m] \quad (8)$$

Where, m^{th} components mole fraction is denoted as x_m, R denotes reheat and the physical exergy of components is determined by eqn. (9)

Physical exergy, $$E_{ph} = h - \sum_m T^*_0 s_m \quad (9)$$

Total exergy, $E = E_{ch} + E_{ph}$ (10)

The thermally operated LiBr/H_2O cooling system evaluations are presented below. The circulation ratio is determined using eqn. (11)

$$\delta = \frac{m^*_s}{m^*_r} = \frac{x_w}{x_s - x_w} \quad (11)$$

$$\Rightarrow \frac{m^*55}{m^*61} = \frac{x_{54}}{x_{55} - x_{54}} \quad (12)$$

Where, m^*_s represents the mass of strong solution, m^*_r denotes the mass of refrigerant, x_w and x_s denotes the concentration of weak and strong solution, respectively. At the absorber, the mass of weak solution is computed using eqn. (13)

$$m^*_w = m^*_s + m^*_r \quad (13)$$

$$\text{i.e., } m^*51 = m^*57 + m^*63 \quad (14)$$

If, m^*_w = 1kg/s, then

$$m^*_r = \frac{m^*_w}{1+\delta} \quad (15)$$

From the exit temperature of HRSG, separator temperature (T_{54}) is determined by eqn. (16)

$$T^*54 = T^*43 - AP \quad (16)$$

The working fluid temperature before throttling is evaluated by eqn. (17)

$$T^*_{56} = T^*_{52} + AP \quad (17)$$

The HEX II energy balance is determined by eqn. (18)

$$h^*_{53} = h^*_{52} + \frac{m^*_{55}(h^*_{55} - h^*_{56})}{m^*_{53}} \quad (18)$$

The concentration of weak solution from generators energy is evaluated by eqn. (19)

$$m^*_{53} = \frac{m^*_{gas}(h^*_{43} - h^*_{44})}{(h^*_{54} - h^*_{53})} \quad (19)$$

The equation of energy balance between evaporator and air cooler is given in eqn. (20)

$$h^*_{31} = h^*_{30} - \frac{m^*_{61}(h^*_{62} - h^*_{61})}{m^*_{air}} \quad (20)$$

The required chilled water mass is determined by eqn. (21)

$$m^*_{cw} = \frac{m^*_{air}(h^*_{30} - h^*_{31})}{P_{c,cw}(T^*_{64} - T^*_{65})} \quad (21)$$

The evaporator's refrigerant mass is computed by eqn. (22)

$$\overset{\circ}{m}{}^*_r = \frac{m_{cw}P_{c,cw}(T^*_{64} - T^*_{65})}{(h^*_{62} - h^*_{61})} \Rightarrow \frac{m_a(h^*_{30} - h^*_{31})}{(h^*_{62} - h^*_{61})} \quad (22)$$

After the generated vapor, the exhaust temperature of gas T^*_{44} can be evaluated from h^*_{44} from eqn. (23)

$$h^*_{44} = h^*_{43} - \frac{m^*_w(h^*_{54} - h^*_{53})}{m^*_e} \quad (23)$$

Where, m^*_e represents the mass of exhaust gas, m^*_{cw} denotes mass of chilled water, and m^*_{air} is the mass of air.

4.2 Process of HACBAS

The HACBAS was proposed to optimize the heat absorber in CCPP to attain the best electricity producing level and cooling capacity. In this research, the novel framework was designed with the combination of Ant Colony [18] optimization (ACO) and Bat optimization (BO) [19]. In ACO, the ant developed a path

between food source and its colony. The distance of path is estimated through pheromone trails, which was leaved from the ant movements randomly. Moreover, in this research, ACO was utilized for energy optimization. Consequently, in BO, the bat were produces a sound to locate their foods. In this, research BO is used for absorbing heat to increase the electricity producing level. In the initial stage process of the probability stage construction is expressed in eqn. (24)

$$R_{k,l}^{*} = \frac{\left(m_{k,l}^{\alpha}\right)\left(w_{k,l}^{\beta}\right)}{\sum\left(m_{k,l}^{\alpha}\right)\left(w_{k,l}^{\beta}\right)} \quad (24)$$

Where, $m_{k,l}$ represents the amount of energy on k,l^{th} components, α denotes the parameter to control the energy $m_{k,l}$ influence, $w_{k,l}$ is the desired energy of k,l^{th} components and β denotes the parameter to control the desired energy $w_{k,l}$ influence. The amount of energy is updated by eqn. (25)

$$m_{k,l} = (1-\delta)m_{k,l} + \Delta m_{k,l} \quad (25)$$

Where, δ is the rate of energy evaporated, $\Delta m_{k,l}$ represents the amount of energy deposited, which is typically given using eqn. (26)

$$\Delta m_{k,l}^{x} = \begin{cases} 1/Q_x & if\ \ energy\ \ distributed\ on\ \ k,l^{th} components \\ 0 & otherwise \end{cases} \quad (26)$$

Where, Q_x is the x^{th} components energy cost (typically length). Moreover, the fitness of BO is added to ACO fitness for enhancing the fitness function. The fitness of bat's movement is expressed by eqn. (27)

$$H_a = H_{min} + \left(H_{max} - H_{min}\right)\alpha \quad (27)$$

$$\Rightarrow m_k^{t+1} = m_k^t + \left(y_k^t - y^*\right)H_a \quad (28)$$

$$\Rightarrow y_k^{t+1} = y_k^t + m_k^t \quad (29)$$

Where, $\alpha \in (0,1)$ denotes the random vector, y^* represents the best heat absorber components among all the components at each iteration t. H_a is the heat absorber velocity increment. In this implementation, we use $H_{min} = 0$ and $H_{max} = O(1)$, based on the domains problem interest size. The generated best solution of heat absorber is expressed in eqn. (30)

$$y_{new} = y_{old} + \in R^t \quad (30)$$

Where, $\in$ denotes the random vector from [-1, 1], R is the average fitness of bat in each iteration. The absorption system's COP is determined as the ratio of absorbed heat by the absorber to the generator's heart rate input is defined in eqn. (31)

$$COP = \frac{H_a}{H_g} \quad (31)$$

Where, H_g represents heat rate of the generator.

The entire process of the proposed HACBAS is explained in the flowchart fig. 4.

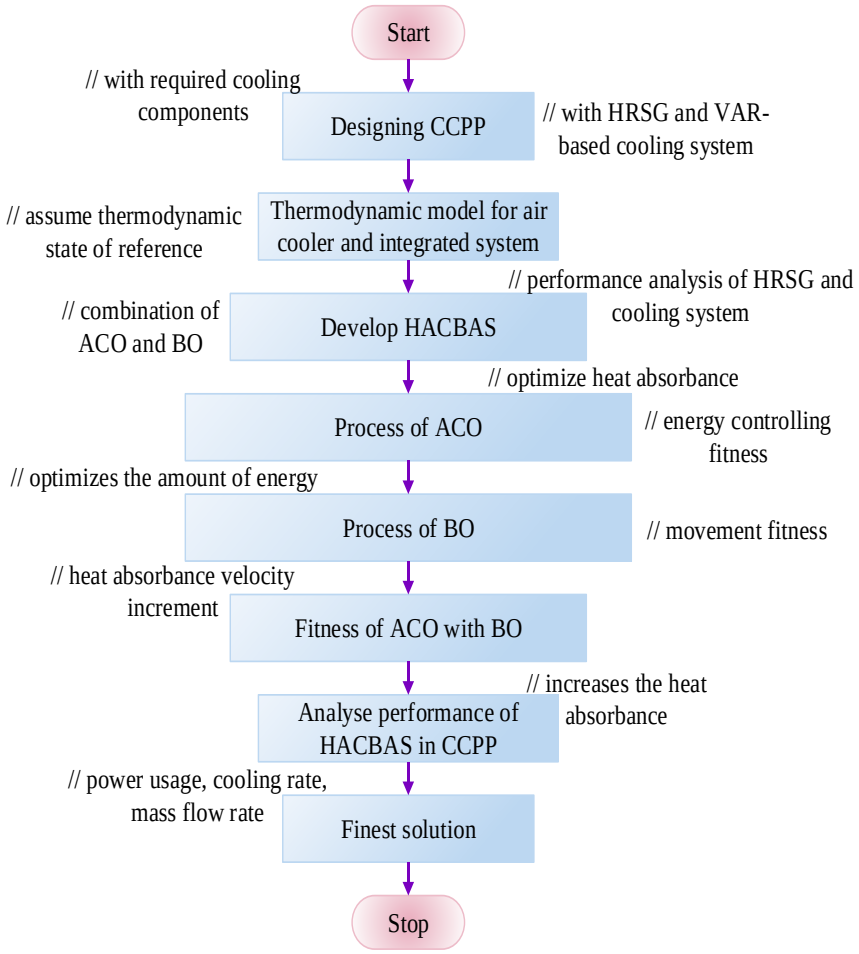

Fig.4 Flowchart of proposed work

At the iteration time, the bat movement is changing, in that the finest outcome is obtained. Moreover, the fitness of each bat is evaluated for the each iteration. The y_{new}, is considered as the best movement of bat. Consequently, the bat updated its movement and moved through the finest path. The best outcome of the bat updated its absorbance capacity.

V. RESULT AND DISCUSSION

The proposed method of CCPP with HRSG and VAR cooling system are executed in the MATLAB/SIMULINK R2018b running on windows 7 platform.

5.1 Case Study

The CCPP with HRSG and VAR cooling system was designed in MATLAB simulation. After designing, a novel HACBAS is implemented to maximize the heat absorbance. Moreover, the assumptions taken for integrated CC evaluation are as follows: The thermodynamic state of reference is taken as 1.01325 bar or 101.325 KPa and 25^0C. The gas cycle maximum temperature and pressure ratio are taken as 1200^0C and 8 respectively. Turbine inlets with HP conditions are taken as 600^0C and 200 bar. The difference between superheated steam and flue gas terminal temperature (TTD) is 25 K. HP and LP economisers approach point (AP) is taken as 15 K and 0.05 bar is considered for condenser pressure.

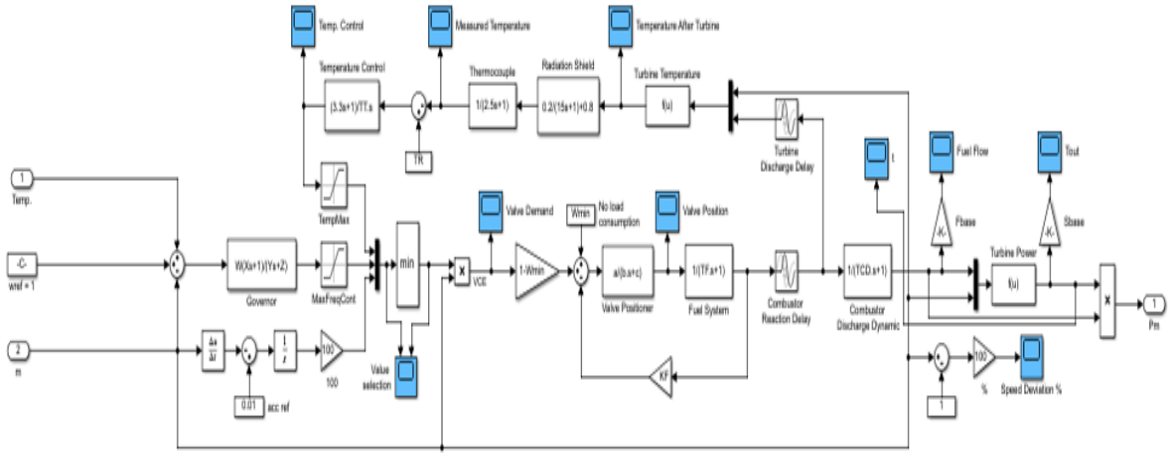

Fig.5 Simulink Gas turbine model

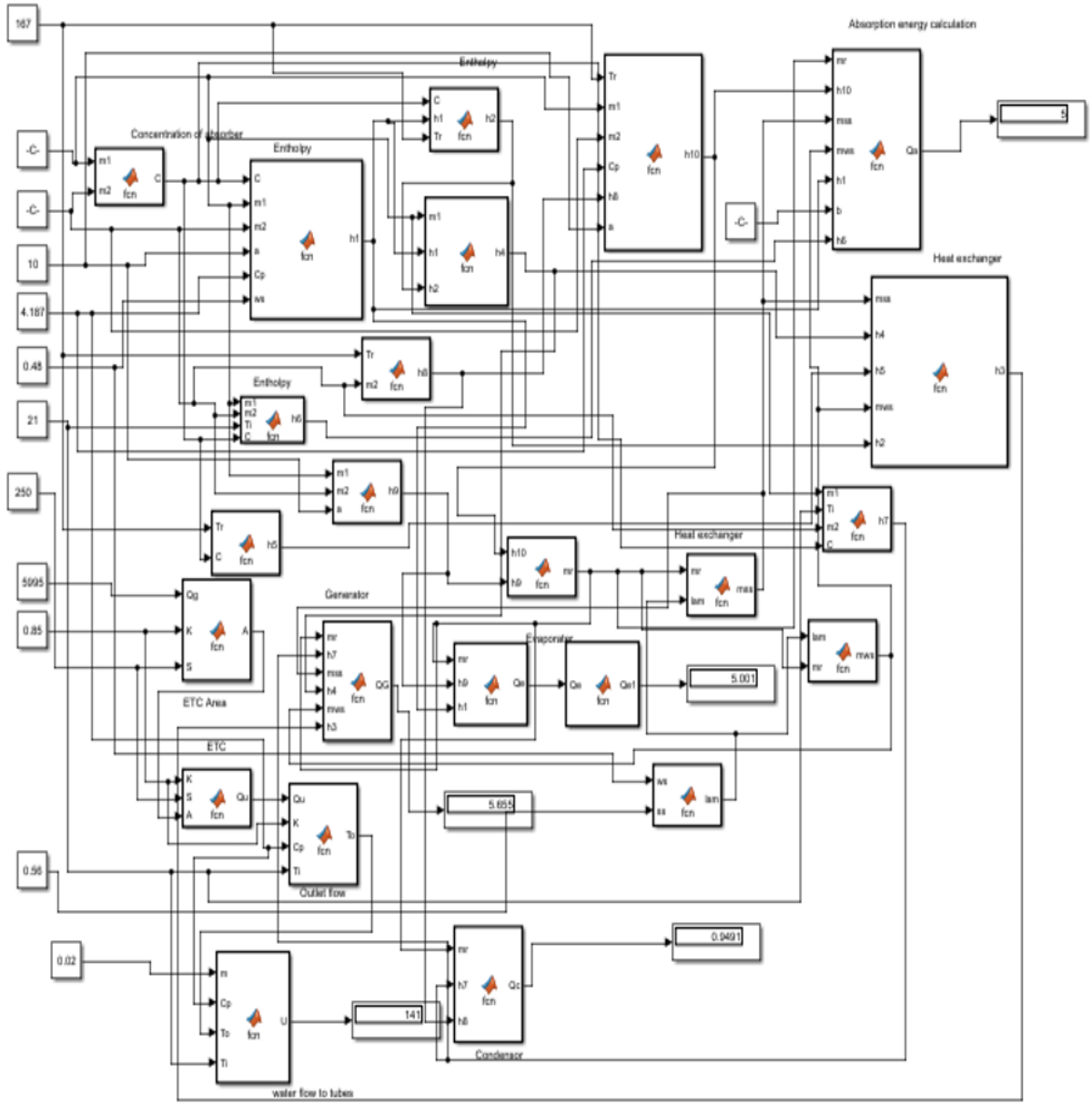

Fig.6 Simulink-HRSG based VAR System

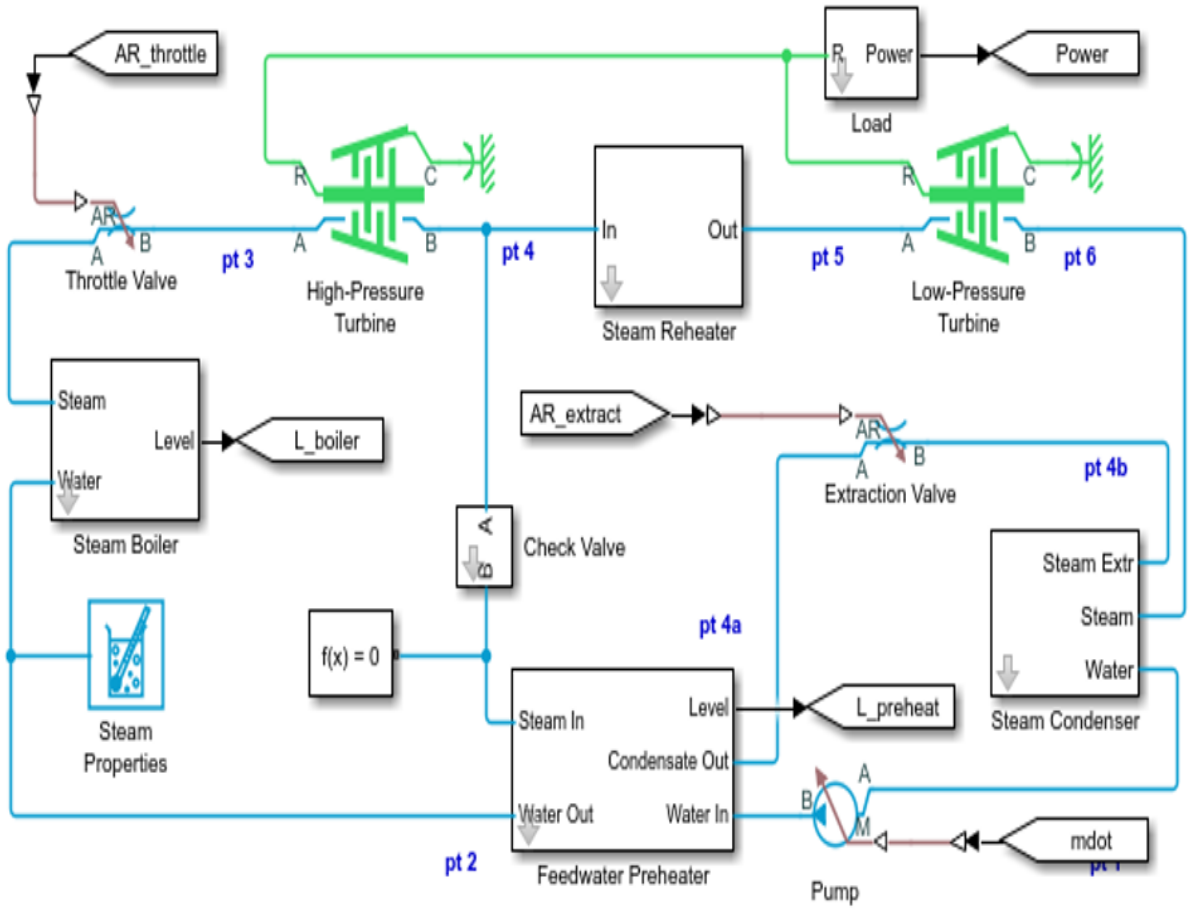

Fig.7 Simulink steam turbine model

The reheat pressure of steam is 50% of high pressure. Pinch point (PP) is described as the minimum difference in temperature between evaporators steam and gas flue is 25 K. In super heater, the degree of superheat (DSH) is considered as 50 K. The GT and compressor efficiency of polytrophic stage is 85%, ST isentropic efficiency is 90%, efficiency of generator is 97% and combustion chamber's pressure drop is 5%. In VAR cooling system, the AP is 5K and absorber and condenser's cooling temperature is taken as 30^0C. HRSG's pressure drop of condenser and deaerator is neglected. Loss of heat in turbines, deaerator, HRSG and condenser is neglected. After the process, the performance is validated with regards of metrics like power usage, thermal efficiency, cooling rate, ambient temperature, mass flow rate, and relative humidity. Moreover, the proposed model was implemented under two different temperatures: 15^0C and 25^0C. The temperatures are varied for climate change; as per Nation Climate Report, the average climate change of year 2022, the temperatures are taken and simulated. The simulation diagram of GT, ST and HRSG model is shown in fig.5, 6 and 7, respectively. The compressor map is shown in fig.8.

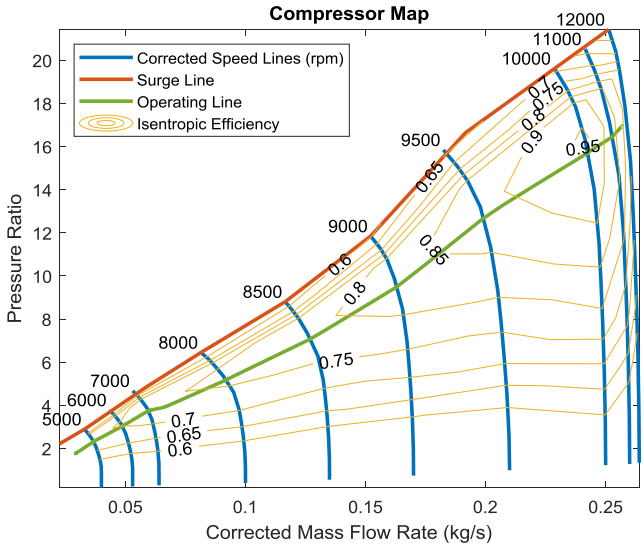

Fig.8 Compressor Map

5.1 Energy flow rate and thermal efficiency

Energy flow rate is defined as the electrical energy per unit time flows through a certain time and it is usually measured in kilowatts (KW) or Watts (W). The CCPP properties at every state points are shown in table.1. The energy flow rate is varied for differed time with respect to its state points.

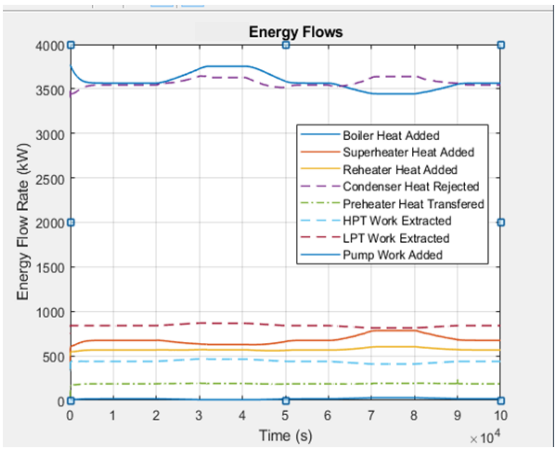

(a)

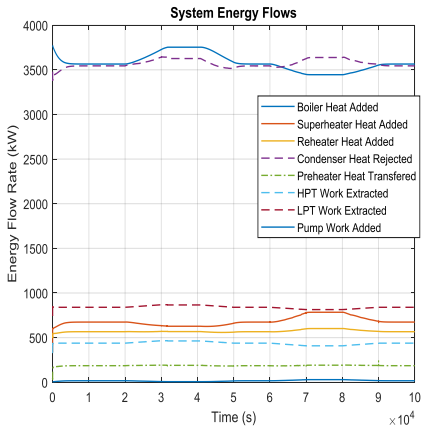

(b)

Fig.9 Energy flow rate vs time (a) at 15^{0}C (b) at 25^{0}C

Table.1 CCPP properties at 15^{0}C air temperature at every state points

State point	Pressure (bar)	Mass flow rate (kg/s)	Temperature (^{0}C)	Enthalpy (kJ/kg)
1	200	16.1	350	2908
2	200	16.1	355	2870
3	210	16	220	2684
4	100	16	210	2655
5	10	15.46	370	2977
6	9.6	15.46	390	2507
7	9.6	15.46	390	2507
8	0.05	16.66	15	2339
11	0.05	16.66	15	2289
12	0.05	16.66	15	2289
13	30	0.1	120	250

14	62	0.13	179	255
15	100	0.3	180	260
16	3.5	9	176	500
17	3.5	9	178	550
18	10	15.46	370	2977
19	10	15.46	370	2977
20	200	8.1	400	2684
21	200	8.1	400	2655
22	8.8	8	400	2685
30	8.8	8	400	2685
31	1.013	551	15	2381
32	1.013	551	15	2386
33	1.013	113	15.018	777
34	1.013	113	15.014	440
35	1.013	113	15.011	435
36	1.013	113	15.008	398
37	1.013	113	15.005	957
38	1.013	113	15.002	352
39	1.013	113	15	312
40	1.013	113	15	227
41	1.013	113	15	181
42	1.013	113	15	153
43	1.013	113	15	75.37
44	1.013	113	15	75.35

The total flow of energy with respect to time is represented in fig.9 and pressure-enthalpy diagram is shown in shown in fig.11.

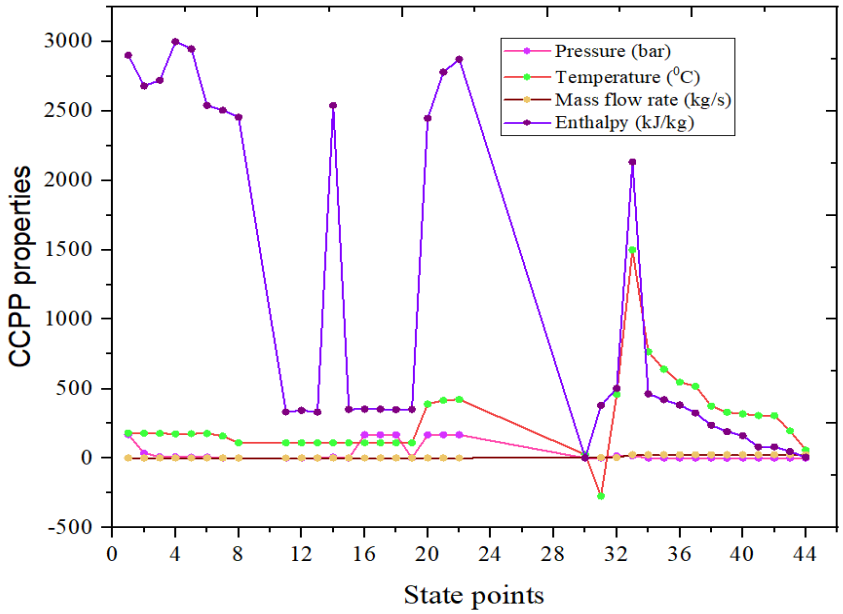

Fig.10 CCPP properties at 25^{0}C air temperature at every state points

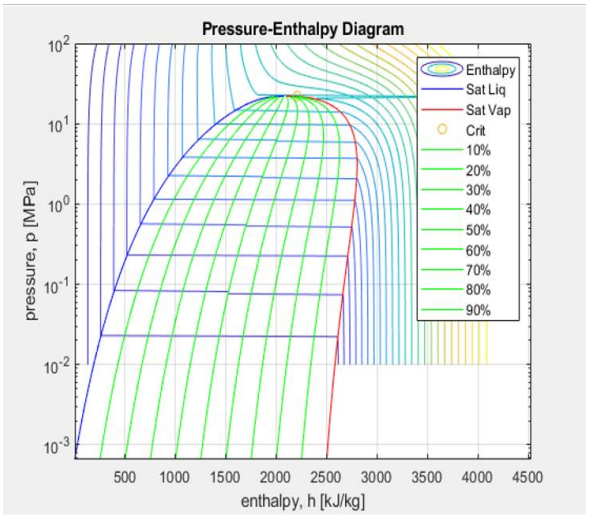

(a)

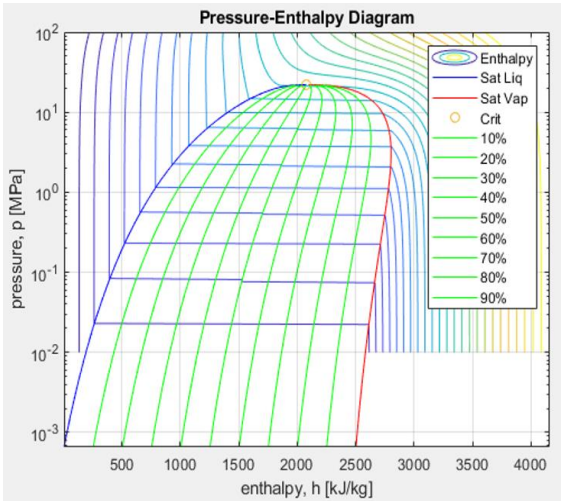

(b)

Fig.11 Pressure-Enthalpy (a) at 15^0C (b) at 25^0C

The thermal efficiency is a device's dimensionless performance measure, which utilizes thermal energy such as furnace, steam turbine, boiler, a refrigerator, and internal-based combustion engine. Moreover, for heat engine, it is described as the fraction of primary heat added that is converted into secondary energy (network output). In refrigeration, it is described as the ratio of total heat output for heating or removal for cooling to input energy. Moreover, the thermal efficiency obtained in the range of 60-96%; it differs for every state points.

5.2 Cooling rate and mass flow rate

The cooling rate is equivalent to the difference between the two objects temperature, multiplied by a constant of material. The unit of cooling rate is degree/unit-time. The cooling plant properties at each state point are shown in table.2.

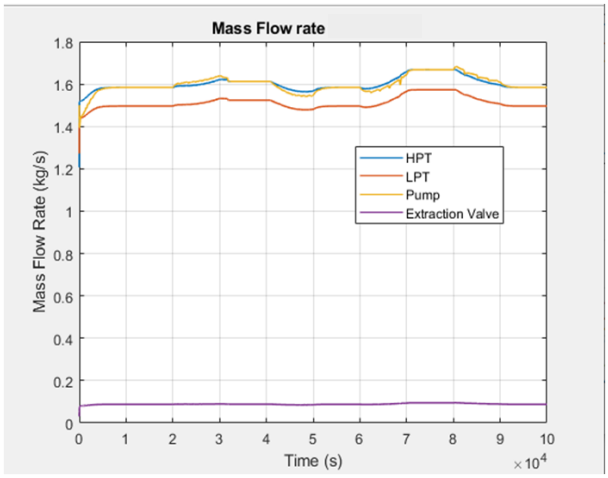

(a)

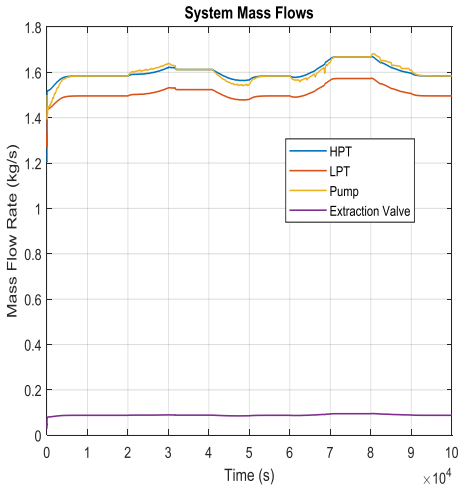

(b)

Fig.12 Mass flow rate vs time (a) at 15^0C (b) at 25^0C

Table.2 cooling plant properties at 15^0C air temperature at each state point

State point	Pressure (bar)	Mass flow rate (kg/s)	Temperature (^{0}C)	Enthalpy (kJ/kg)
51	0.654	0.02403	13.5	160
52	0.654	0.02403	13.5	165
53	0.654	0.02403	13.5	168
54	0.285	0.0245	55	117
55	0.285	0.0245	57	176
56	0.285	0.0245	75	175.46
57	0.285	0.0245	140	117

58	0.285	5	149	170
59	0.654	5	127	155
60	0.285	5	35	176
61	0.85	5.001	30	2450.80
62	0.85	5.655	21	147
63	0.9	18.02	-37.5	115.30
64	0.9	18.02	-37.5	2606.65
65	1.01	18.02	-37.5	-31.72

The mass flow rate is defined as the mass passing per unit time. It is directly dependent on the liquid velocity, cross-section area and density. Its unit is kgs^{-1}. The mass flow rate vs time are shown in fig.12.

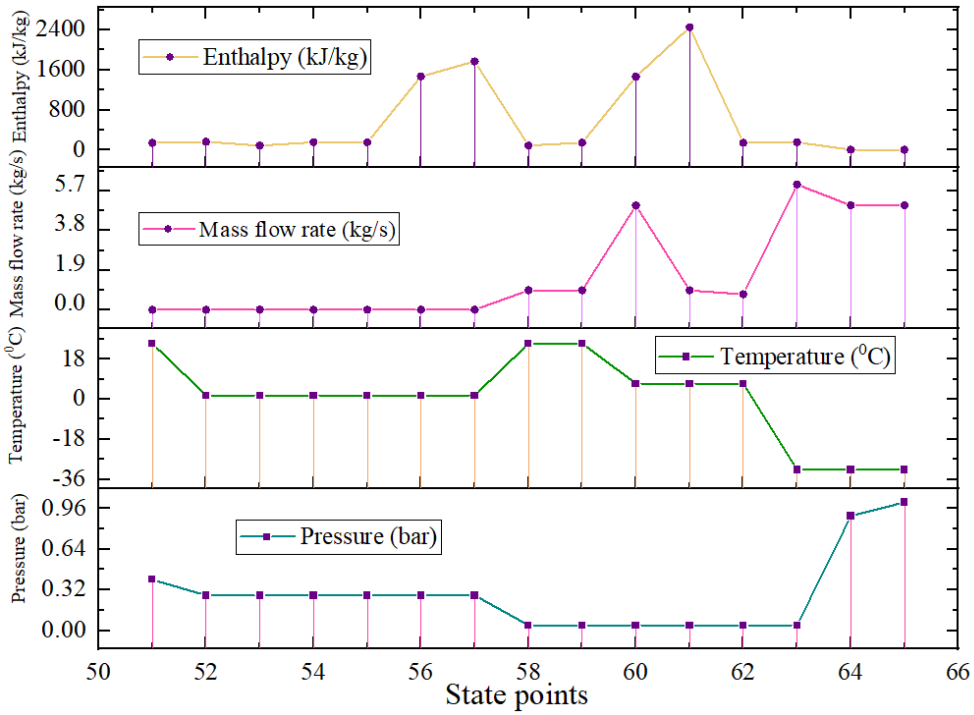

Fig.13 cooling plant properties at 25^{0}C air temperature at each state point

The results indicate that plant effectiveness is greatest when the ratio of compressor pressure is set to 8 at a 1,200°C combustion temperature. When the ratio of compressor pressure is greater than 10, then cooling method is preferred. When contrasted to the structure without cooling, cooling outcomes of inlet air in a high energy output in all equivalence ratios.

5.3 Ambient temperature and relative humidity

The CCPP performance was strongly based on the ambient temperature. It is defined as the environment or objects air temperature of equipment is stored. Moreover, when the ambient temperature rises, the total power generated in the CCPP decreases and the heat increases i.e. decreases the efficiency.

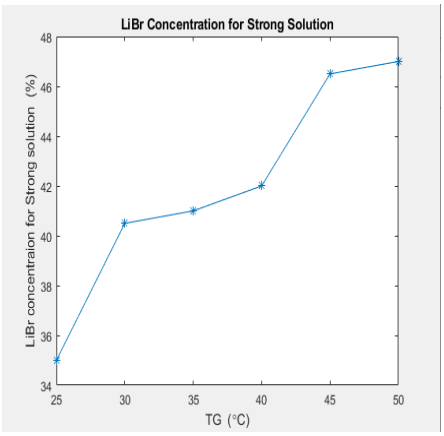

(a)

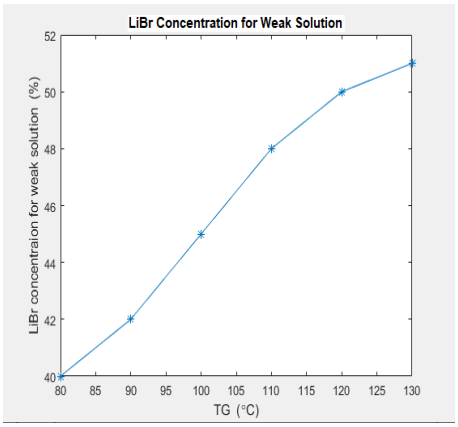

(b)

Fig.14 LiBr concentration (a) strong solution (b) weak solution

The Lithium Bromide (LiBr) concentration for both weak and strong solution is shown in fig.14. The graph of temperature vs entropy is shown in fig.15. The inlet air temperature of compressor is differed from 14°C to 30°C, and the ratio of compressor pressure is changed from 7 to 16. Even without option of air cooling, air is conceded at 30°C, implying that the air coolant is circumvented. Moreover, the ambient temperature is 12-33^{0}C for the developed CCPP.

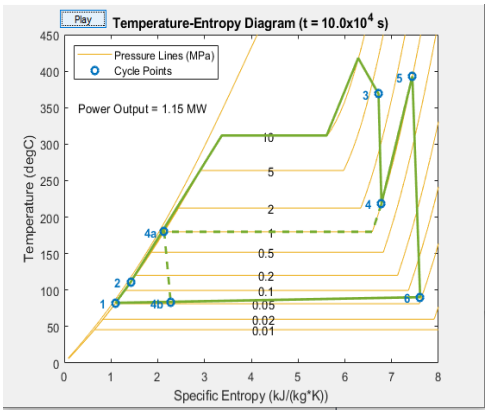

(a)

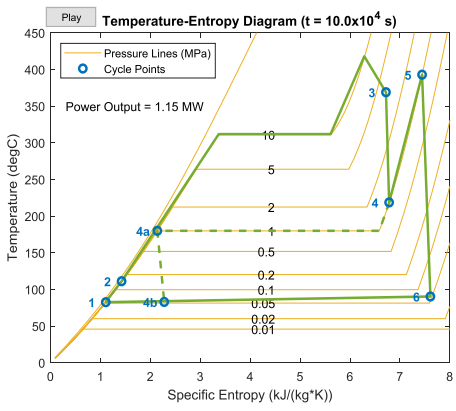

(b)

Fig.15 Temperature vs Entropy (a) at 15^{0}C (b) at 25^{0}C

Relative humidity is described as the ratio of total water vapor actually presented in air to the greatest possible amount at the same temperature. Its unit is %, and it is also described as the ratio between the moisture amounts in the air at a particular temperature to the maximum moisturized air can withstand at the same temperature. The relative humidity obtained by the presented approach is 50% and 100%.

5.4 Comparative analysis of Coefficient of performance (COP)

The co-efficient of performance (COP) measures the amount of heat energy moved in contrast to the amount of used heat energy. Moreover, the presented model has attained the COP as 0.97. Further, to identify the effectiveness of the presented method, the COP was compared with existing techniques like automated MPFHE and Renewable CCPP. Furthermore, the obtained COP for the presented model is shown in fig.16.

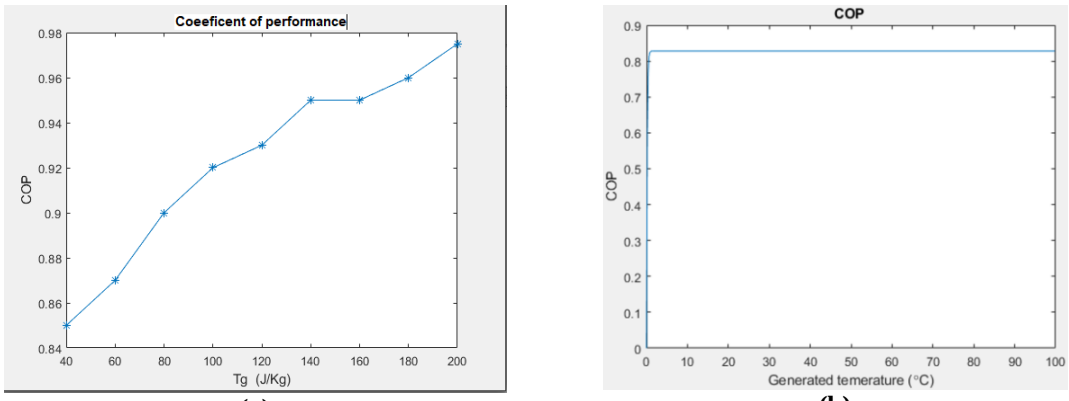

(a) **(b)**

Fig.16 Obtained COP (a) at 15^0C (b) at 25^0C

Table.3 Coefficient of performance comparison

Sl.no	Technique	Coefficient of performance
1	Automated MPHFE	1.694
2	Renewable CCPP	2.96
3	Proposed	0.97

By comparing with other models, the presented model has attained higher COP. The automated MPHE has attained the COP as 1.694 and renewable CCPP has attained the COP as 2.96. For working fluid, the presented thermophysical properties increase the exit temperature and drop the COP than other models.

VI. CONCLUSION

In this paper, the Combined Cycle Power Plant (CCPP) and Vapour Absorption Refrigeration cooling system is designed in MATLAB simulation. A single-effect-based Lithium Bromide-water ($LiBr/H_2O$) VAR cooling system was designed based on thermodynamic process. The heat absorbance was optimized by developing Hybrid Ant Colony Bat Absorber System (HACBAS). The performance of the system is validated with regards of power usage, ambient temperature, relative humidity, thermal efficiency, mass flow rate and cooling rate. The study suggests that, with an accurate thermodynamic analysis and theoretical design there is a scope for improving the heat absorbance performance. The presented optimization minimizes the environmental impacts, generates minimum amount of secondary wastes, which are sustainable, based on future and current social and economic needs. Further, the presented model has rational energy use, reduces energy consumption and losses.

REFERENCE

[1]. Madadian, Edris, Jan B. Haelssig, Mina Mohebbi, and Michael Pegg. "From biorefinery landfills towards a sustainable circular bioeconomy: A techno-economic and environmental analysis in Atlantic Canada." Journal of Cleaner Production 296 (2021): 126590.
[2]. Madadian, Edris, et al. "From biorefinery landfills towards a sustainable circular bioeconomy: A techno-economic and environmental analysis in Atlantic Canada." Journal of Cleaner Production 296 (2021): 126590.
[3]. Ferry, Jonathan, Bennett Widyolar, Lun Jiang, and Roland Winston. "Solar thermal wastewater evaporation for brine management and low pressure steam using the XCPC." Applied Energy 265 (2020): 114746.
[4]. Jiang, Long, et al. "Post-combustion CO2 capture from a natural gas combined cycle power plant using activated carbon adsorption." Applied Energy 245 (2019): 1-15.
[5]. Mohammadi, Kasra, Kevin Ellingwood, and Kody Powell. "A novel triple power cycle featuring a gas turbine cycle with supercritical carbon dioxide and organic Rankine cycles: Thermoeconomic analysis and optimization." Energy Conversion and Management 220 (2020): 113123.
[6]. Arabkoohsar, Ahmad. "Combination of air-based high-temperature heat and power storage system with an Organic Rankine Cycle for an improved electricity efficiency." Applied Thermal Engineering 167 (2020): 114762.
[7]. Salehi, Mirhamed, et al. "Analysis and prediction of gas turbine performance with evaporative cooling processes by developing a stage stacking algorithm." Journal of Cleaner Production 277 (2020): 122666.
[8]. Karatas, Yalcin, and DenizYilmaz. "Experimental investigation of the microclimate effects on floating solar power plant energy efficiency." Clean Technologies and Environmental Policy (2021): 1-14.
[9]. Deng, Chao, et al. "Air cooling techniques and corresponding impacts on combined cycle power plant (CCPP) performance: A review." International Journal of Refrigeration (2020).
[10]. Gado, Mohamed G., Shinichi Ookawara, Sameh Nada, and Ibrahim I. El-Sharkawy. "Hybrid sorption-vapor compression cooling systems: A comprehensive overview." Renewable and Sustainable Energy Reviews 143 (2021): 110912.
[11]. Alklaibi, A. M., &Lior, N. (2021). Waste heat utilization from internal combustion engines for power augmentation and refrigeration. Renewable and Sustainable Energy Reviews, 152, 111629.
[12]. Khaliq ,Dincer , et al. "Air cooling techniques and corresponding impacts on combined cycle power plant (CCPP) performance" , 2020-Elsevier
[13]. Peng, Wei, and OmidKarimiSadaghiani. "Presentation of an Integrated Cooling System for enhancement of Cooling Capability in Heller Cooling Tower with Thermodynamic Analyses and Optimization." International Journal of Refrigeration (2021).

[14]. Ahmad, Adnan Darwish, Ahmad M. Abubaker, Yousef SH Najjar, and Yaman Mohammad Ali Manaserh. "Power boosting of a combined cycle power plant in Jordan: An integration of hybrid inlet cooling & solar systems." Energy Conversion and Management 214 (2020): 112894.
[15]. Malar, A., et al. "Multi constraints applied energy efficient routing technique based on ant colony optimization used for disaster resilient location detection in mobile ad-hoc network." Journal of Ambient Intelligence and Humanized Computing 12.3 (2021): 4007-4017.
[16]. Cao, Yan, et al. "Multi-objective bat optimization for a biomass gasifier integrated energy system based on 4E analyses." Applied Thermal Engineering 196 (2021): 117339.
[17]. Srinivas, T., and D. Vignesh. "Performance enhancement of GT-ST power plant with inlet air cooling using lithium bromide/water vapour absorption refrigeration system." International journal of energy technology and policy 8.1 (2012): 94-107.
[18]. Allahyarzadeh-Bidgoli, Ali, Daniel Jonas Dezan, and Jurandir Itizo Yanagihara. "COP optimization of propane pre-cooling cycle by optimal Fin design of heat exchangers: Efficiency and sustainability improvement." Journal of Cleaner Production 271 (2020): 122585.
[19]. Seyam, Shaimaa, Ibrahim Dincer, and Martin Agelin-Chaab. "Development of a clean power plant integrated with a solar farm for a sustainable community." Energy Conversion and Management 225 (2020): 113434.

Mude Murali Mohan Naik, et. al. "Performance Analysis of Combined Cycle Power Plant with Inlet Air Cooling System." *IOSR Journal of Mechanical and Civil Engineering (IOSR-JMCE),* 20(2), 2023, pp. 42-57.